

Theory of Ionic Polymer Conductor Network Composite

Xiao Wang (王霄)¹ and Wei Hong (洪伟)^{2,1*}

¹Department of Materials Science and Engineering, Iowa State University, Ames, IA 50011, USA

²Department of Aerospace Engineering, Iowa State University, Ames, IA 50011, USA

*whong@iastate.edu

Abstract

Ionic polymer conductor network composite (IPCNC) is a mixed conductor consisting of a network of loaded ionomer and another network of metallic particles. It is known that the microstructure of the composite, especially that of the electrodes, plays a dominating role in the performance of an IPCNC. However the microstructures of IPCNC have seldom been addressed in theoretical models. This letter formulates a continuum field theory for IPCNC by considering a supercapacitor-like microstructure with a large distributed interface area. The theory is then applied to the study of the equilibrium deformation and electrochemistry in a thin-sheet IPCNC actuator.

A variety of ionic polymer conductor network composites (IPCNCs, including the ionic polymer metal composite) have been developed as soft actuators and sensors in the past decade.¹⁻⁶ A widely accepted mechanism pictures the IPCNC as an ionomer thin film sandwiched between two flat electrodes and assumes it to be homogeneous and purely ionic conductive.⁷⁻¹⁰ Upon application of a low voltage, the mobile ions in the ionomer undergo directional motions: cations migrate towards the cathode while anions migrate towards the anode. The actuator bends as a consequence of the charge accumulation near the electrode surfaces,^{9,11,12} and the magnitude of deformation could be controlled electrically.

However such an idealization may lead to problematic predictions. As a conductor, the homogeneous ionomer is electroneutral in equilibrium or in a steady state, except in the very thin boundary layer (i.e. the electric double layer) near the ionomer-electrode interface. The electric double layer, at a typical thickness of \sim nm for aqueous solutions, is too thin to effectively bend the IPCNC with a thickness of \sim 100 μ m. Moreover, the estimated electric capacitance of IPCNC as a parallel capacitor is much lower than measured.^{11,13-15} Many models circumvent these discrepancies by introducing a dielectric constant much higher than that of deionized water,^{11,16,17} while the physical origin of this fitting parameter remains unclear. These difficulties may be resolved by realizing that the IPCNC electrodes are made from precipitating nano metal particles into the bulk polymer even in the early designs.^{13,18} As a result, the active domain extends deep into the bulk even though the boundary layer near the particle-matrix interface is still very thin. The capacitance boost can thus be explained from the large interfacial area.^{12,19} Corrections have been made on the parallel-plate model to account for the finite roughness of

electrodes.^{12,20} The dependence on specific microstructures limits the application of these modified models, especially when the electrodes undergo a drastic change in design.^{2,3} The lack of predictive power of current modeling tools has already hindered the further development and scale-up of IPCNCs.

Following an approach similar to that used in polyelectrolyte gels,²¹ this letter develops an equilibrium field theory by considering IPCNC as a mixed conductor. Due to the complexity of the system, the discussion is limited to the effect of electric double layer on electro-mechanical coupling among various other processes.^{11,16} Instead of the commonly accepted parallel-plate-capacitor picture, let us consider a tri-layer model as sketched in Fig. 1. Two layers of composite consisting of both the ionic conductive phase (ICP) and the electronic conductive phase (ECP) are connected to a battery, and the middle layer is simply ionic conductive. The spatially distributed ECP provides a large interfacial area, similar to the structure of a supercapacitor. Both the length scale of the microstructures and that of the electric double layer on the interface between the two phases are assumed to be small compared to the overall size of the device, so that a homogenized continuum model can be deduced.

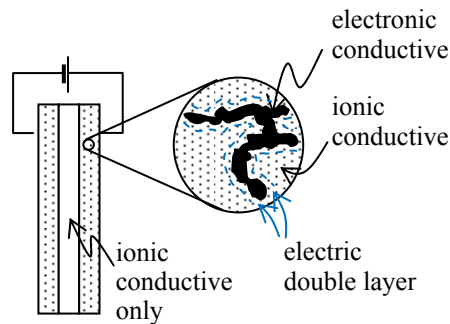


Fig. 1 A tri-layer model of an IPCNC actuator. The two composite electrode layers are mixed conductors and have finite thickness.

There are usually two ways of doing work to an IPCNC: by exerting a field of mechanical forces and by applying a field of electric voltage. Associated with a change in displacement field $\delta \mathbf{u}(\mathbf{x})$, the field of mechanical tractions $\mathbf{t}(\mathbf{x})$ on a surface does work $\int t_i \delta u_i dA$. Imagine connecting to the IPCNC a field of batteries with potential $\Phi(\mathbf{x})$. Through injection of electrons $\delta q(\mathbf{x})$ into the IPCNC, the battery field does electric work $\int \Phi \delta q dV$, where $q(\mathbf{x})$ is the concentration of electronic charge in the volume. Let W be the Helmholtz free energy per unit volume of the IPCNC. Unlike general polyelectrolyte gels, an IPCNC usually operates in an environment from which the exchange of mobile species is prevented.²² Therefore the total number of each mobile species is conserved. Let $c_+(\mathbf{x})$ and $c_-(\mathbf{x})$ be the concentrations of mobile cations and anions respectively. The conservation of species requires that

$\int c_{\pm} dV = N_{\pm}$, where N_{\pm} is the total number of mobile ions, a known constant for each IPCNC. We enforce this constraint by adding to the total free energy of the system a term, $\mu_{\pm}(N_{\pm} - \int c_{\pm} dV)$, with μ_{\pm} being a Lagrange multiplier for each type of mobile ions. In equilibrium, the change in the Helmholtz free energy of the IPCNC equals the work done by the external agents:

$$\int \delta W dV - \mu_+ \int \delta c_+ dV - \mu_- \int \delta c_- dV = \int t_i \delta u_i dA + \int \Phi \delta q dV, \quad (1)$$

for arbitrary changes in displacement $\delta \mathbf{u}$ and electronic charge density $\delta q(\mathbf{x})$.

Now let us turn to a representative homogenized material particle in the IPCNC. Large volumetric change is of less interest to most IPCNC applications, since the material is preserved from dehydration during operation. With thin-film bending as the common mode of deformation, the material is only slightly strained. We thus take the as-swollen stress-free state as the reference, and use the small strain tensor $\varepsilon_{ij} = \frac{1}{2}(\partial u_i / \partial x_j + \partial u_j / \partial x_i)$ to represent the field of deformation. While detailed microstructures of material particles may differ from each other, the state of a material particle is fully determined by the homogenized fields of deformation, electronic charge density, and ion concentrations. Writing the free energy function as $W(\boldsymbol{\varepsilon}, c_+, c_-, q)$, we have

$$\delta W = \frac{\partial W}{\partial \varepsilon_{ij}} \delta \varepsilon_{ij} + \frac{\partial W}{\partial c_+} \delta c_+ + \frac{\partial W}{\partial c_-} \delta c_- + \frac{\partial W}{\partial q} \delta q. \quad (2)$$

Assuming molecular incompressibility, the concentration of solvent c_s is no longer an independent state variable, but related to the volumetric strain as $v_s c_s - v_s \bar{c}_s = \varepsilon_{kk}$, where v_s is the volume of a solvent molecule and \bar{c}_s is the reference solvent concentration.

As a conductor, an IPCNC in equilibrium is electroneutral except for the thin electric double layer on interfaces. The representative material particle contains both ICP and ECP, and the total charge (electronic and ionic) is zero. Following Newmann and Tobias²³, we assume the electroneutrality in an equilibrium state:

$$q + e(c_+ - c_- - c_0) = 0, \quad (3)$$

where e is the elementary charge and c_0 the concentration of fixed ions. Without losing generality, it is assumed that the fixed ions on ionomer carry negative charge, and all ions have either -1 or $+1$ valence. Utilizing Eqs. (1)-(3) and the divergence theorem, we arrive at the following equilibrium equations:

$$\frac{\partial}{\partial x_j} \left(\frac{\partial W}{\partial \varepsilon_{ij}} \right) = 0, \quad (4)$$

$$\mu_{\pm} = \pm e \left(\Phi - \frac{\partial W}{\partial q} \right) + \frac{\partial W}{\partial c_{\pm}}. \quad (5)$$

One may recognize that Eq. (4) recovers the familiar form of mechanical equilibrium equation when the stress $\sigma_{ij} = \partial W / \partial \varepsilon_{ij}$ is defined. If we introduce an effective electric potential, $\Phi' = \Phi - \partial W / \partial q$, Eq. (5) will have the same form as the electrochemical potentials in an open system. However, μ_{\pm} in Eq. (5) is the Lagrange multiplier to be determined from the conservation equation, $\int c_{\pm} dV = N_{\pm}$. The effective potential Φ' may be regarded as the effective electric potential of the homogenized material particle.

Once a specific material model is prescribed in terms of the free-energy function W , the inhomogeneous field of deformation and ion-distribution can be solved from the algebraic-differential system, Eqs. (4) and (5). For the purpose of illustration, we use a free-energy function in the form:

$$W = \frac{E}{2(1+\nu)} \left(\varepsilon_{ij} \varepsilon_{ij} + \frac{\nu}{1-2\nu} \varepsilon_{kk} \varepsilon_{jj} \right) + \frac{1}{2} \frac{q^2}{AK} + kT \left(c_+ \ln \frac{c_+}{c_+ + c_- + c_s} + c_- \ln \frac{c_-}{c_+ + c_- + c_s} + c_s \ln \frac{c_s}{c_+ + c_- + c_s} \right). \quad (6)$$

The first term on the right-hand side of Eq. (6) is the elastic energy with E being Young's modulus and ν Poisson's ratio. The second term is the contribution from the electric double layers. Here a linear capacitor model is adopted for the electrostatic energy of the double layers, in which K is a material parameter defined as the capacitance per unit area of interface, and A a microstructural parameter representing the area of the interfaces contained per unit volume of the IPCNC. The combination AK characterizes the electronic-charge-storage capability of the IPCNC. The last term in Eq. (6) is the energy of mixing mobile ions and the solvent, and only the entropic contribution is taken into account. kT is the temperature of the system in the unit of energy.

Applying the specific form of free energy function to the equations of state, we obtain that

$$\sigma_{ij} = \frac{E}{1+\nu} \left(\varepsilon_{ij} + \frac{\nu}{1-2\nu} \varepsilon_{kk} \delta_{ij} \right) - \frac{kT}{v_s} \ln \left(\frac{c_s + c_+ + c_- \bar{c}_s}{\bar{c}_s + \bar{c}_+ + \bar{c}_- c_s} \right) \delta_{ij}, \quad (7)$$

$$\mu_{\pm} = \pm e \left[\Phi - \frac{kT}{e\gamma} \left(\frac{c_+}{c_0} - \frac{c_-}{c_0} - 1 \right) \right] + kT \ln \frac{c_{\pm}}{c_+ + c_- + c_s}, \quad (8)$$

where \bar{c}_{\pm} and \bar{c}_s are the concentrations of the mobile ions and solvent molecules in the reference state respectively. The second term on the right-hand side of Eq. (7) is due to the coupling between volumetric strain and the solvent concentration, and is often referred to as the osmotic pressure P . A dimensionless parameter, $\gamma = kTAK/e^2c_0$, which characterizes the relative capacitance of the electric double layers on the distributed interface of an IPCNC, can be identified in this model. In the limit when $\gamma \rightarrow 0$, the IPCNC reduces to a pure ICP, in which the effective potential Φ' equals the macroscopically measurable potential Φ . At the two mixed conductor layers, γ takes a higher value. Using a typical volume fraction 1% for metal particles, and the size range of the particles 1nm~100nm, we have an estimate of the interfacial area density $A \approx 10^5 \sim 10^7 \text{m}^{-1}$. Using the representative value for the double-layer capacitance $K \approx 0.1 \sim 1 \text{Fm}^{-2}$ ²⁴ and a fixed-charge concentration $c_0 \approx 1\text{M}$, we further estimate that $\gamma \approx 10^{-5} \sim 10^{-2}$. Inspired by the measurement of the metal-particle distribution,¹¹ we assume that γ decreases linearly from both surfaces in the mixed conductor layers and vanishes in the middle layer.

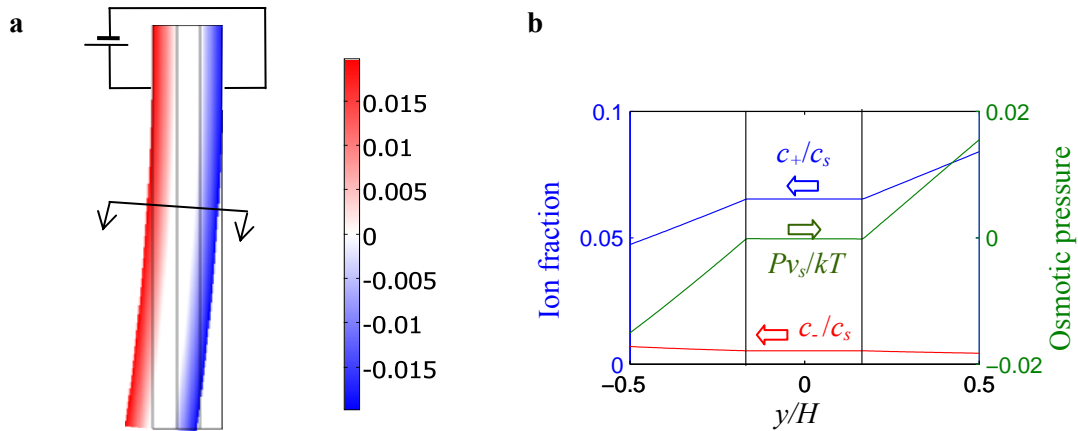


Fig. 2 a) The bending of an ICP under applied electric voltage. The color scale shows the concentration of electronic charge on ECP where blue denotes negative charge and red denotes positive charge. **b)** The distributions of counterions (blue) and coions (red) and that of the resulting osmotic pressure through the thickness of the bending ICP.

The numerical solution to the differential-algebraic system, Eqs. (4) and (5), by using the commercial finite-element software COMSOL 3.5a, is shown in Fig. 2. Corresponding to a Nafion 117 with 50% volume increase when swollen by a solution of concentration 1M, parameters used in this example are: fixed-charge density $c_0 = 1.7\text{M}$, reference ion concentrations $\bar{c}_+ = 1.8\text{M}$ and $\bar{c}_- = 0.1\text{M}$, reference solvent concentration $\bar{c}_s = 28\text{M}$, and the microstructure parameter $\gamma = 5 \times 10^{-4}$ on the two surfaces of the IPCNC. The mixed conductor layers each take one third of the total thickness. The driving force for bending of the IPCNC is the asymmetrically distributed osmotic pressure resulting from the biased ion distributions. Due to the Donnan exclusion effect, the available counterions are more abundant than the

co-ions.²⁵ The normalized osmotic pressure, pv_s/kT , is evenly distributed through the thickness of the IPCNC, as shown in Fig. 2b., rather than being concentrated near the surfaces. The peak value of the normalized osmotic pressure, ~ 0.01 , is also at a much more reasonable order of magnitude than those from parallel-capacitor models.

Detailed mechanisms aside, the deformation of IPCNC is driven by the inhomogeneous fields in the electric double layers as a result of ion and solvent migration. When the distributed interface area is accounted for through the microstructure parameter γ , the characteristic length of the effective layer is no longer the Debye length but naturally determined by the distribution of the ECP.

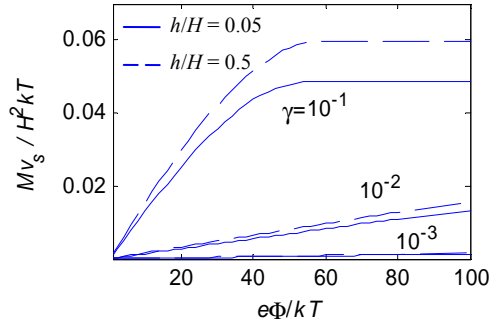


Fig. 3 The blocking moment of an IPCNC as a function of the normalized voltage. On the surfaces, the dimensionless parameter which characterizes the distributed interfacial area, $\gamma = 10^{-1}, 10^{-2}, 10^{-3}$ and decreases linearly through the mixed conducting layers. The thicknesses of the mixed conducting layer are 5% (solid curves) or 50% (dashed curves) of the whole IPCNC sheet.

Now let us estimate the blocking moment of a thin sheet of IPCNC by constraining its deformation. Integrating the moment of the axial stress σ_{yy} yields the moment per unit width needed to block the bending of an IPCNC:

$$M = \int_{-H/2}^{H/2} \frac{kT}{v_s} \ln \left(\frac{c_s + c_+ + c_- \bar{c}_s}{\bar{c}_s + \bar{c}_+ + \bar{c}_- c_s} \right) y dy, \quad (9)$$

where H is the thickness of the IPCNC sheet. The blocking moments of two IPCNCs with different mixed-conductor-layer thicknesses are plotted in Fig. 3. The influence of the microstructure is also shown with various values of the dimensionless parameter γ . The blocking moment increases almost linearly with the applied potential. If we neglect chemical reactions, with certain density of fixed charges, there also exists a limiting blocking moment. This limit corresponds to the maximum response of an IPCNC, when the mobile counterions are depleted near the anode as shown by plateau of the $\gamma = 0.1$ curve. The existing IPCNCs often have very small γ , so that this limit is hardly reached when a small electric potential is applied. Nevertheless, the results show that redesigning the microstructure of the mixed conductor layers for a higher γ value (e.g. by using finer metal particles or using layer-by-layer

deposition) or simply thickening the mixed conductive layers will greatly enhance the performance of an IPCNC.

In summary, a continuum theory is developed to answer the following question: How could the inhomogeneous fields which are localized within nanometers from interfaces drive a macroscopic IPCNC film? While the basic physics is not altered and the electric double layers remain to be nanometer thick, the microstructure of the mixed conductive IPCNC provides a spatially distributed interfacial area which results in a much thicker active actuation zone. Through a microstructure parameter that captures the capacitance of the distributed double layers, the field theory is capable of predicting the coupling behaviors of IPCNCs, and more importantly correlating their performance with the underlying microstructures. Although the model presented includes the electromechanical coupling through osmotic effect only, the field theory developed herein can be easily extended to include other mechanisms, such as the clustered ion pairs.^{2,18} As the interfacial area between different conductive phases increases, all mechanisms whose effects depend on the inhomogeneity in the double layers would also be greatly enhanced.

The authors acknowledge the support from the National Science Foundation through Grant No. CMMI-0900342, and Prof. Q. M. Zhang at Penn State University for the valuable discussions.

References

- ¹K. Asaka, K. Oguro, Y. Nishimura, M. Mizuhata and H. Takenaka, *Polym. J.* **27** (4), 436-440 (1995).
- ²S. Liu, R. Montazami, Y. Liu, V. Jain, M. R. Lin, X. Zhou, J. R. Heflin and Q. M. Zhang, *Sensor Actuator A* **157** (2), 267-275 (2010).
- ³I. K. Oh and J. Y. Jung, *J. Intel. Mater. Syst. Struct.* **19** (3), 305-311 (2008).
- ⁴M. D. Bennett and D. J. Leo, *Sensor Actuator A* **115** (1), 79-90 (2004).
- ⁵M. Uchida and M. Taya, *Polymer* **42** (22), 9281-9285 (2001).
- ⁶Y. Bar-Cohen, S. Leary, M. Shahinpoor, J. O. Harrison and J. Smith, *Smart Structures and Materials 1999: Electroactive Polymer Actuators and Devices* **3669**, 51-56
- ⁷M. Shahinpoor, *Smart Structures and Materials 1999: Electroactive Polymer Actuators and Devices* **3669**, 109-121
- ⁸B. J. Akle and D. J. Leo, *Smart Mater. Struct.* **16** (4), 1348-1360 (2007).
- ⁹K. Asaka and K. Oguro, *J. Electroanal. Chem.* **480** (1-2), 186-198 (2000).
- ¹⁰Y. Bar-Cohen and Q. M. Zhang, *MRS Bull.* **33** (3), 173-181 (2008).
- ¹¹S. Nemat-Nasser, *J. Appl. Phys.* **92** (5), 2899-2915 (2002).
- ¹²M. Aureli, W. Y. Lin and M. Porfiri, *J. Appl. Phys.* **105** (10), - (2009).

- ¹³B. J. Akle, M. D. Bennett, D. J. Leo, K. B. Wiles and J. E. McGrath, *J. Mater. Sci.* **42** (16), 7031-7041 (2007).
- ¹⁴S. J. Kim, S.-M. Kim, K. J. Kim and Y. H. Kim, *Smart Mater. Struct.* **16** (6), 2286-2295 (2007).
- ¹⁵Y. Liu, S. Liu, J. H. Lin, D. Wang, V. Jain, R. Montazami, J. R. Heflin, J. Li, L. Madsen and Q. M. Zhang, *Appl. Phys. Lett.* **96** (22), - (2010).
- ¹⁶T. Wallmersperger, D. J. Leo and C. S. Kothera, *J. Appl. Phys.* **101** (2), - (2007).
- ¹⁷D. Pugal, K. J. Kim, A. Punning, H. Kasemagi, M. Kruusmaa and A. Aabloo, *J. Appl. Phys.* **103** (8), - (2008).
- ¹⁸K. Onishi, S. Sewa, K. Asaka, N. Fujiwara and K. Oguro, *Electrochim. Acta* **46** (5), 737-743 (2000).
- ¹⁹X. Q. Bao, Y. Bar-Cohen and S. S. Lih, *Smart Structures and Materials 2002: Electroactive Polymer Actuators and Devices* **4695**, 220-227
- ²⁰F. Gao and L. M. Weiland, *Smasis2008: Proceedings of the ASME Conference on Smart Materials, Adaptive Structures and Intelligent Systems - 2008, Vol 1*, 259-264
- ²¹W. Hong, X. H. Zhao and Z. G. Suo, *J. Mech. Phys. Solids* **58** (4), 558-577 (2010).
- ²²D. Pugal, K. Jung, A. Aabloo and K. J. Kim, *Polymer International* **59** (3), 279-289 (2010).
- ²³J. S. Newman and C. W. Tobias, *J. Electrochem. Soc.* **109** (8), C193-C193 (1962).
- ²⁴B. E. Conway, *Electrochemical supercapacitors : scientific fundamentals and technological applications*. (Plenum Press, New York, 1999).
- ²⁵F. G. Donnan, *Chem. Rev.* **1** (1), 73-90 (1924).